Letters

IOP Publishing

Journal of Physics A: Mathematical and Theoretical

J. Phys. A: Math. Theor. **53** (2020) 09LT01 (14pp)

https://doi.org/10.1088/1751-8121/ab6af0

**Letter**

# Exact stationary state of a run-and-tumble particle with three internal states in a harmonic trap

**Urna Basu[1], Satya N Majumdar[2], Alberto Rosso[2], Sanjib Sabhapandit[1] and Grégory Schehr[2,3]**

[1] Raman Research Institute, Bengaluru 560080, India
[2] LPTMS, CNRS, Univ. Paris-Sud, Université Paris-Saclay, 91405 Orsay, France

E-mail: gregory.schehr@u-psud.fr

Received 24 October 2019, revised 18 December 2019
Accepted for publication 13 January 2020
Published 4 February 2020

**Abstract**

We study the motion of a one-dimensional run-and-tumble particle with three discrete internal states in the presence of a harmonic trap of stiffness $\mu$. The three internal states, corresponding to positive, negative and zero velocities respectively, evolve following a jump process with rate $\gamma$. We compute the stationary position distribution exactly for arbitrary values of $\mu$ and $\gamma$ which turns out to have a finite support on the real line. We show that the distribution undergoes a shape-transition as $\beta = \gamma/\mu$ is changed. For $\beta < 1$, the distribution has a double-concave shape and shows algebraic divergences with an exponent $(\beta - 1)$ both at the origin and at the boundaries. For $\beta > 1$, the position distribution becomes convex, vanishing at the boundaries and with a single, finite, peak at the origin. We also show that for the special case $\beta = 1$, the distribution shows a logarithmic divergence near the origin while saturating to a constant value at the boundaries.

Keywords: stochastic processes, active particles, exact solution

(Some figures may appear in colour only in the online journal)

## 1. Introduction

Recent years have seen a surge of interest in the study of active matter and active particles. The term 'active particle' refers to a class of self-propelled particles which can generate dissipative directed motion by consuming energy directly from their environment [1–6]. Examples of active matter can be found in nature at all length scales, ranging from micro-organisms

[3] Author to whom any correspondence should be addressed.

  

like bacteria [7, 8] to granular matter [9, 10], flock of birds [11, 12] and fish-schools [13, 14]. Apart from a diverse set of novel collective behaviours like clustering [15–18], motility induced phase separation [19–21], and absence of well defined pressure [22], active particles show many intriguing features even at the single particle level. One such interesting feature is that, in the presence of external potentials and confining boundaries, active particles show very different behaviour than their passive counterparts, including non-Boltzmann stationary state, clustering near the boundaries of the confining region [23–29] and unusual relaxation and persistence properties [30–32]. There have been numerous recent studies focusing on the behaviour of active particles in the presence of external potentials and confinements, both theoretical [33–36] and experimental [37–40].

The theoretical attempts to characterise the behaviour of active particles focus on studying simple models of such systems. Run-and-tumble particle (RTP) is one such class of models which mimics the motion of certain bacteria which moves via alternating straight runs and random tumbling events resulting in reorientations.In its simplest version, an RTP is an over-damped particle which moves with a constant speed $v_0$, or 'runs,' along the direction of an internal 'spin' degree of freedom. The orientation of the spin can change randomly resulting in a sudden change, or 'tumble,' in the direction of motion of the particle. Several variations and generalizations of this simple RTP dynamics have been studied in the recent literature including finite tumble durations [41–43], space dependent speed [44] and effect of interactions [45–47].

The most studied example of the RTP dynamics is in one spatial dimension where the internal spin can assume two possible values $\sigma = \pm 1$. In this case, the particle moves with velocity $v_0$ or $-v_0$; the reversal of direction occurs stochastically with rate $\gamma$, with the flipping of the spin $\sigma \to -\sigma$. In the presence of an external potential $U(x)$, the position $x(t)$ of this two-state RTP evolves according to the Langevin equation,

$$\dot{x} = f(x) + v_0\sigma(t) \tag{1}$$

where $f(x) = -U'(x)$ is the deterministic force acting on the particle. The spin variable $\sigma$ plays the role of the noise, its dichotomous nature giving rise to the 'activity'. In fact, it is clear from the auto-correlation $\langle \sigma(t)\sigma(t')\rangle = \mathrm{e}^{-2\gamma|t-t'|}$ that $\sigma(t)$ is a coloured noise with a finite memory, characterised by the persistence time $\tau = (2\gamma)^{-1}$. Despite the apparent simplicity of the model, the two-state RTP shows a lot of intriguing features typical to active particles including non-Boltzmann stationary distribution [24, 30].

For any confining potential, the stationary position distribution of a two-state RTP is known exactly, and is given by,

$$P_{\rm st}(x) \propto \frac{1}{v_0^2 - f^2(x)} \exp\left[2\gamma \int_0^x \mathrm{d}y \frac{f(y)}{v_0^2 - f^2(y)}\right] \tag{2}$$

up to a normalization constant. The above result was first obtained long ago in the context of quantum optics [48–51], and later to study the role of coloured noise in dynamical systems [52]. More recently, it has been re-derived in the context of active particles [22, 24]. In particular, the stationary distribution (2) has been analysed for specific confining potentials of the type $U(x) \propto |x|^p$ with $p > 0$ in [24]. The case $p = 2$ corresponds to a harmonic potential which is of particular interest, not only from theoretical but also from an experimental point of view [38, 40]. For a harmonic potential $U(x) = \mu x^2/2$, the stationary distribution (2) simplifies to,

$$P_{\rm st}(x) = \frac{2\mu}{4^\beta B(\beta,\beta) v_0} \left[1 - \left(\frac{\mu x}{v_0}\right)^2\right]^{\beta-1} \tag{3}$$

where $\beta = \gamma/\mu$ and $B(u, v)$ is the beta-function. This distribution is symmetric in $x$ and has a finite support in the region $-\frac{v_0}{\mu} \leqslant x \leqslant \frac{v_0}{\mu}$. Consequently, the particle is confined within this region in the stationary state. This stationary position distribution shows an interesting shape-transition as a function of $\beta$. For $\beta > 1$ the distribution is convex shaped, with a peak at the origin $x = 0$ and $P_{\rm st}(x)$ vanishing at the boundaries $x = \pm\frac{v_0}{\mu}$. On the other hand, for $\beta < 1$ $P_{\rm st}(x)$ has a concave shape with divergences at the boundaries and a minimum at the origin. For $\beta = 1$, the distribution is uniform. Thus by varying $\beta$, one can observe a transition from a double-peaked (at the boundaries) to a single-peaked distribution. The double-peaked nature of the distribution for $\gamma < \mu$ signifies an 'active phase', where the persistence time of the spin-orientation is larger than $\mu^{-1}$, the relaxation time-scale of the potential. On the other hand, $\gamma > \mu$, i.e. when the persistence time is smaller compared to $\mu^{-1}$, corresponds to a passive phase, where the stationary distribution resembles that of a passive particle in a trap, with a single peak at the centre of the trap. Indeed, in the diffusive limit when $v_0 \to \infty$, $\gamma \to \infty$ but keeping the ratio $v_0^2/2\gamma = D$ fixed, the dynamics of the RTP in the harmonic trap converges to the Ornstein–Uhlenbeck process[4]. This is also exhibited in the stationary state where the distribution in equation (3) converges to a Boltzmann distribution, which in this case is a simple Gaussian $P_{\rm st}(x) \propto {\rm e}^{-\frac{\mu}{D}x^2}$.

It is then natural to ask how the stationary distribution changes if the RTP has more than two internal states. In fact, an RTP with many internal degrees have been studied where the internal degrees can take a set of discrete values and evolve following some discrete jump processes [53, 54]. However, most of these studies are numerical and to the best of our knowledge no analytical results are available for the stationary state of a multi-state RTP in the presence of an external potential.

In this article, we study a run-and-tumble active particle in one spatial dimension with three discrete internal states, with positive, negative and zero velocities, respectively. We show that such a multi-state dynamics naturally arises when one considers an RTP in higher spatial dimensions and project it to one-dimension. We calculate exactly the stationary position probability distribution $P(x)$ in the presence of a harmonic potential of strength $\mu$ for arbitrary flip-rate $\gamma$ among the internal states. It turns out that, similar to the two-state case, $P(x)$ has a finite support on the real line and its shape is governed by a single dimensionless parameter

$$\beta = \frac{\gamma}{\mu}. \tag{4}$$

Note that $\beta$ is the ratio of the two time-scales present in the system, namely, the relaxation time $\mu^{-1}$ in the trap and $\gamma^{-1}$, the time-scale associated with the flipping of the internal spin. The parameter $\beta$ acts as a measure of the 'activity' of the dynamics. For small $\beta$, i.e. when the persistence time $\gamma^{-1}$ is much larger than the relaxation time scale $\mu^{-1}$, one would expect strong effects of activity such as non-Boltzmann stationary states, while in the opposite limit the dynamics resembles more of a normal diffusive particle in a trap leading to Boltzmann-like stationary state. Such a transition in the stationary state as the parameter $\beta$ is increased has been demonstrated recently in the 2-state RTP model in a confining potential in one dimension as discussed above [24], as well as in 2-d active Brownian motion model in the presence of a harmonic trap [25]. In this paper, our exact solution for the 3-state RTP model demonstrates a similar transition in the stationary position distribution $P(x)$ from an 'active' like shape to a 'passive' like shape as the activity parameter $\beta$ increases through $\beta = 1$. For $\beta < 1$, $P(x)$

[4] Note that the Ornstein–Uhlenbeck process here refers to the dynamics of the position $x(t)$ (and not the velocity $v(t)$) of an overdamped Brownian particle in the presence of a harmonic trap: it is not the standard Ornstein–Uhlenbeck process $v(t)$ describing the evolution of the velocity of an inertial particle in the presence of friction and noise.

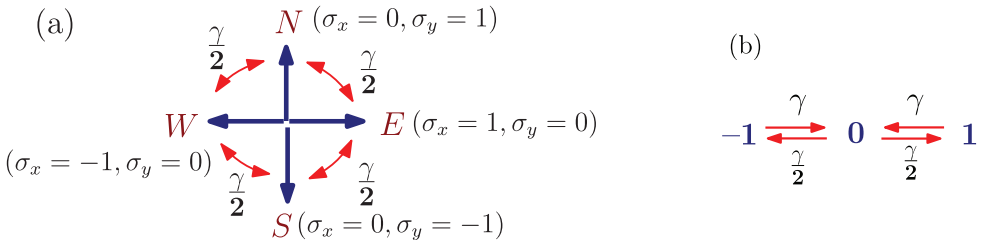


**Figure 1.** (a) Schematic representation of the jump process through which the orientation $\sigma$ evolves. (b) The equivalent 3-state jump process for $\sigma_x$.

diverges both at the origin and the boundaries with the same exponent $\beta - 1$. Thus, in this case, the position distribution has a double-concave shape, with three peaks, namely at the boundaries and the origin. For $\beta = 1$, $P(x)$ shows a logarithmic divergence near the origin. On the other hand, for $\beta > 1$, the distribution converges to a finite value at the origin while it vanishes at the boundaries, implying a convex shape with a single peak at the origin (see figure 2).

## 2. Model

Our model of a three-state RTP in one-dimension is motivated by a natural 'clock-like' model for a two-dimensional RTP. In the standard RTP model in 2-d the orientation angle is continuous $\theta \in [0, 2\pi]$; the particle moves along a direction $\theta$ with constant speed during a run until $\theta$ changes via a tumbling event. A natural variation of this model is where the orientation $\theta$ can have only certain discrete values. This is similar in spirit to spin systems where 'clock' models are the natural discrete analogue of Heisenberg models with a continuous spin degree of freedom. Here we show that while the continuous-$\theta$ RTP model in the presence of a 2-d harmonic trap is still not solvable analytically for the stationary state, a particular discrete version of this model is tractable analytically. Let us consider an overdamped particle moving on a two dimensional $(xy)$ plane with an internal orientational degree of freedom or 'spin' $\sigma$ associated with it. In the absence of any external potential the particle moves with a constant speed $v_0$ along the direction of $\sigma$, which is a unit vector with four possible discrete orientations, denoted by $E, W, N, S$ (along $\pm x$ and $\pm y$ axes respectively). The spin $\sigma$ evolves in time following a Markov jump process—its orientation can change via a rotation of $\frac{\pi}{2}$ either clockwise or anti-clockwise, both with rate $\frac{\gamma}{2}$. This jump process is schematically represented in figure 1(a). Additionally, we consider an external harmonic potential $U(x, y) = \frac{\mu}{2}(x^2 + y^2)$ which exerts a force $f(x, y) = -\nabla U(x, y)$ on the RTP.

The time-evolution of the position $(x(t), y(t))$ of the RTP can be conveniently expressed in terms of the Langevin equations,

$$\dot{x}(t) = -\mu x(t) + v_0 \sigma_x(t) \tag{5a}$$

$$\dot{y}(t) = -\mu y(t) + v_0 \sigma_y(t) \tag{5b}$$

where $\sigma_{x,y}(t)$ are components of the spin vector $\sigma(t)$ at any time $t$, along the $x$ and $y$ axes respectively (see figure 1(a)).

The position probability distribution $\mathcal{P}(x, y, t)$ is given by the sum $\mathcal{P}(x, y, t) = \sum_\sigma \mathcal{P}_\sigma(x, y, t)$ where $\mathcal{P}_\sigma(x, y, t)$ denotes the probability that the particle has the position $(x, y)$ and orientation $\sigma = E, N, W, S$ at time $t$. These probabilities evolve according to the Fokker–Planck (FP) equations,

$$\frac{\partial}{\partial t}\mathcal{P}_E(x,y,t) = \frac{\partial}{\partial x}\Big[(\mu x - v_0)\mathcal{P}_E\Big] + \frac{\partial}{\partial y}\Big[\mu y \mathcal{P}_E\Big] + \frac{\gamma}{2}(\mathcal{P}_N + \mathcal{P}_S) - \gamma \mathcal{P}_E \tag{6a}$$

$$\frac{\partial}{\partial t}\mathcal{P}_N(x,y,t) = \frac{\partial}{\partial x}\Big[\mu x \mathcal{P}_N\Big] + \frac{\partial}{\partial y}\Big[(\mu y - v_0)\mathcal{P}_N\Big] + \frac{\gamma}{2}(\mathcal{P}_E + \mathcal{P}_W) - \gamma \mathcal{P}_N \tag{6b}$$

$$\frac{\partial}{\partial t}\mathcal{P}_W(x,y,t) = \frac{\partial}{\partial x}\Big[(\mu x + v_0)\mathcal{P}_W\Big] + \frac{\partial}{\partial y}\Big[\mu y \mathcal{P}_W\Big] + \frac{\gamma}{2}(\mathcal{P}_N + \mathcal{P}_S) - \gamma \mathcal{P}_W \tag{6c}$$

$$\frac{\partial}{\partial t}\mathcal{P}_S(x,y,t) = \frac{\partial}{\partial x}\Big[\mu x \mathcal{P}_S\Big] + \frac{\partial}{\partial y}\Big[(\mu y + v_0)\mathcal{P}_S\Big] + \frac{\gamma}{2}(\mathcal{P}_E + \mathcal{P}_W) - \gamma \mathcal{P}_S \tag{6d}$$

where we have suppressed the argument of $\mathcal{P}_\sigma$ on the right hand side for the sake of brevity. It is hard to find an analytical form of $\mathcal{P}(x,y,t)$ as these equations are difficult to solve, even in the stationary state.

However, it is also interesting to look at the $x$-process only, governed by equation (5*a*). This describes an effective one-dimensional RTP where the internal spin $\sigma_x$ has three possible discrete values, $1, 0, -1$. As illustrated in figure 1(a), both $\sigma = N$ and $\sigma = S$ correspond to $\sigma_x = 0$ while $\sigma = E$ and $\sigma = W$ corresponds to $\sigma_x = 1$ and $\sigma_x = -1$, respectively. The jump from $\sigma_x = 1$ to 0 can, thus, occur through two different channels ($E \to N$ and $E \to S$), resulting in a jump rate $\gamma$ for $\sigma_x = 1 \to \sigma_x = 0$. Similarly, $\sigma_x = -1 \to \sigma_x = 0$ also occurs with rate $\gamma$. On the other hand, the transition $\sigma_x = 0 \to 1$ corresponds to the jumps $\sigma = N \to E$ and $\sigma = S \to E$; since, at any given time, the particle with $\sigma_x = 0$ can be in only one of the source states $N$ and $S$, the effective rate for the transition $0 \to 1$ is $\gamma/2$. Similarly, the effective transition rate for $0 \to -1$ is also $\gamma/2$. This effective 3-state jump process in one-dimension is schematically shown in figure 1(b). Let $P_i(x,t)$ denote the probability that the RTP is at a position $x$ at time $t$ with $\sigma_x = i$. The corresponding FP equations read,

$$\frac{\partial}{\partial t}P_1(x,t) = \frac{\partial}{\partial x}[(\mu x - v_0)P_1] + \frac{\gamma}{2}P_0 - \gamma P_1 \tag{7a}$$

$$\frac{\partial}{\partial t}P_{-1}(x,t) = \frac{\partial}{\partial x}[(\mu x + v_0)P_{-1}] + \frac{\gamma}{2}P_0 - \gamma P_{-1} \tag{7b}$$

$$\frac{\partial}{\partial t}P_0(x,t) = \frac{\partial}{\partial x}[\mu x P_0] + \gamma(P_1 + P_{-1}) - \gamma P_0. \tag{7c}$$

We note that this set of FP equations can also be obtained from equations (6*a*)–(6*d*) by integrating both sides over $y$ and then identifying $P_1(x,t) = \int \mathrm{d}y\ \mathcal{P}_E(x,y,t)$, $P_{-1}(x,t) = \int \mathrm{d}y\ \mathcal{P}_W(x,y,t)$, and $P_0(x,t) = \int \mathrm{d}y\ [\mathcal{P}_N(x,y,t) + \mathcal{P}_S(x,y,t)]$.

In the presence of the confining harmonic potential, in the long time limit the RTP is expected to reach a stationary state where the left hand side (l. h. s.) of the equations (7*a*)–(7*c*) would vanish. The corresponding stationary distributions $P_i(x) = \lim_{t\to\infty} P_i(x,t)$ then satisfy a set of coupled linear differential equations (obtained by putting $\frac{\partial P_i}{\partial t} = 0$),

$$\frac{\mathrm{d}}{\mathrm{d}x}[(\mu x - v_0)P_1] + \frac{\gamma}{2}P_0 - \gamma P_1 = 0 \tag{8a}$$

$$\frac{\mathrm{d}}{\mathrm{d}x}[(\mu x + v_0)P_{-1}] + \frac{\gamma}{2}P_0 - \gamma P_{-1} = 0 \tag{8b}$$

$$\frac{\mathrm{d}}{\mathrm{d}x}[\mu x P_0] + \gamma(P_1 + P_{-1}) - \gamma P_0 = 0. \tag{8c}$$

Our objective is to solve this set of equations to find $P_i(x)$ in the stationary state.

**Boundary Conditions.** While at any finite time $t$ equations (7*a*)–(7*c*) hold in the full space $x \in [-\infty, \infty]$, the steady state equations (8*a*)–(8*c*) hold only over a finite domain $x \in [x_-, x_+]$, where $x_\pm = \pm v_0/\mu$. This is because in the stationary state the RTP gets trapped in this finite interval $x \in [x_-, x_+]$. This can be understood easily from the following argument: from the Langevin equation (5*a*) it is clear that if the particle is outside the region $[x_-, x_+]$, it always feels a drift towards the origin, irrespective of the value of $\sigma_x$. As a result, if the particle starts from some initial position $x_0 > x_+$, or $x_0 < x_-$, it will eventually reach the region $[x_-, x_+]$. Consequently, the stationary distribution has a finite support in the region $[x_-, x_+]$ and it is zero outside.

To solve the stationary equations (8*a*)–(8*c*) in the finite segment $x \in [x_-, x_+]$, we need to specify the boundary conditions at the two endpoints $x_-$ and $x_+$. These boundary conditions have to be provided additionally, and can not be obtained via discretising the original equations (7*a*)–(7*c*) near $x_\pm$. To derive these additional boundary conditions we need to investigate the trajectory near the boundary points $x_\pm$. For this purpose, let us first look at the behaviour of $P_1(x)$ at $x = x_-$. To find $P_1(x_-, t)$, i.e. the probability that the particle is at $x = x_-$ at time $t$, we have to consider the trajectory of the particle during the infinitesimal interval $[t - \Delta t, t]$—during this interval the particle (i) either moved a distance $\Delta x = (-\mu x_- + v_0)\Delta t + O(\Delta t^2)$ (see the Langevin equation (5*a*)) with $\sigma_x = 1$ or (ii) $\sigma_x$ flipped from $0 \to 1$ while the position did not change. The probabilities for these run and the tumbling events are $(1 - \gamma\Delta t)$ and $\gamma\Delta t/2$, respectively. Then, one can write,

$$P_1(x_-, t + \Delta t) = (1 - \gamma\Delta t)P_1(x_- - \Delta x, t) + \frac{\gamma}{2}\Delta t P_0(x_-, t). \tag{9}$$

Let us emphasize again that this equation is not a discretized version of the FP equation (7*a*) near $x = x_-$, rather it has to be derived separately in the stationary state. Now, in the stationary state, the probabilities $P_i(x)$ are independent of time, hence, we have from (9),

$$P_1(x_-) = (1 - \gamma\Delta t)P_1(x_- - \Delta x) + \frac{\gamma}{2}\Delta t P_0(x_-). \tag{10}$$

Moreover, from equation (5*a*) we have, for $\sigma_x = 1$ and near $x_-$, $\Delta x = (-\mu x_- + v_0)\Delta t = 2v_0\Delta t > 0$, thus $P_1(x_- - \Delta x) = P_1(x_- - 2v_0\Delta t)$ which vanishes in the stationary state, as the argument $x_- - 2v_0\Delta t$ is outside the region $[x_-, x_+]$. Then, taking $\Delta t \to 0$ limit in equation (10), we get $P_1(x_-) = 0$. Using similar arguments for $P_{-1}$ and $P_0$, one finds the full set of boundary conditions to be satisfied by the set of equations (8*a*)–(8*c*),

$$P_1(x_-) = 0,\ P_{-1}(x_+) = 0,\ P_0(x_-) = 0,\ P_0(x_+) = 0. \tag{11}$$

Note that the behaviour of $P_1(x_+)$ and $P_{-1}(x_-)$ remain unspecified and we will see that these boundary conditions (11) are enough to uniquely determine the stationary state. The set of boundary conditions for $P_1$ and $P_{-1}$ is very similar to the case of 2-state RTP [24]. However, as we will see below, the presence of the third state $\sigma_x = 0$ leads to a richer behaviour in the present case.

## 3. Exact solution

The straightforward strategy to solve a set of coupled first order equations like equations (8*a*)–(8*c*) is to decouple them and find separate equations for $P_i(x)$. However, our primary goal is to find the marginal position distribution of the particle, i.e. the probability that the effective one-dimensional RTP has a position $x$, irrespective of the spin-orientation $\sigma_x$. This is given by

$$P(x) = P_0(x) + P_1(x) + P_{-1}(x). \tag{12}$$

In the following we attempt to derive an equation for $P(x)$ using equations (8*a*)–(8*c*). To this end, we first define,

$$Q(x) = P_1(x) + P_{-1}(x), \quad \text{and} \quad R(x) = P_1(x) - P_{-1}(x). \tag{13}$$

It is straightforward to see that in terms of these functions $P$ and $Q$, the four boundary conditions given by equation (11) translate to,

$$P(x_+) = Q(x_+), \quad \text{and } P(x_-) = Q(x_-). \tag{14}$$

Note that the boundary conditions of $R(x)$ remain unspecified.

We proceed by expressing equations (8*a*)–(8*c*) in terms of these functions $P$ and $Q$. For this purpose, we first add equations (8*a*)–(8*c*) to get,

$$\frac{\mathrm{d}}{\mathrm{d}x}\Big[\mu x P(x) - v_0 R(x)\Big] = 0 \;\Rightarrow \mu x P(x) - v_0 R(x) = C \tag{15}$$

where $C$ is a constant independent of $x$. To determine $C$, we substitute $x = x_+$ in the above equation. Using the definitions of $P$ and $R$, along with the boundary condition (11), we get, $C = (\mu x_+ - v_0)P_1(x_+) = 0$. Hence, from equation (15) we have,

$$R(x) = \frac{\mu x}{v_0} P(x) \tag{16}$$

for all values of $x$. Now, adding equations (8*a*) and (8*b*) and using equation (16), we get,

$$\mu x P'(x) + (\mu - \gamma)P(x) = \mu x Q'(x) + (\mu - 2\gamma)Q(x) \tag{17}$$

where $'$ denotes the derivative with respect to (w.r.t.) the argument of the functions. Next, we subtract equation (8*b*) from equation (8*a*) to get,

$$(\mu x)^2 P'(x) + \mu(2\mu - \gamma)xP(x) = v_0^2 Q'(x). \tag{18}$$

Equations (17) and (18) are two coupled linear differential equations involving $P(x)$ and $Q(x)$. In the following, we use them to get two separate differential equations for $P(x)$ and $Q(x)$. But, first, it is convenient to use a change of variable $z = (\frac{\mu x}{v_0})^2$ with $0 \leqslant z \leqslant 1$. Let us denote $\tilde{P}(z) = P(x = v_0\sqrt{z}/\mu)$ and $\tilde{Q}(z) = Q(x = v_0\sqrt{z}/\mu)$. Equations (17) and (18) then become,

$$2z\tilde{P}'(z) + (1 - \beta)\tilde{P}(z) = 2z\tilde{Q}'(z) + (1 - 2\beta)\tilde{Q}(z) \tag{19}$$

$$z\tilde{P}'(z) + \left(1 - \frac{\beta}{2}\right)\tilde{P}(z) = \tilde{Q}'(z) \tag{20}$$

where $\beta = \gamma/\mu$. The two boundary conditions in equation (14) reduce to a single condition for $\tilde{P}$ and $\tilde{Q}$,

$$\tilde{P}(z = 1) = \tilde{Q}(z = 1). \tag{21}$$

As we will see below, this boundary condition is enough to solve the differential equations uniquely.

To get an equation involving $\tilde{P}(z)$ only, we take derivative of equation (19) w.r.t. $z$. Then, using equation (20), we immediately arrive at a second order differential equation,

$$z(1-z)\tilde{P}''(z) + \left[\frac{3-\beta}{2} - \frac{1}{2}(7-3\beta)z\right]\tilde{P}'(z) - \left(1-\frac{\beta}{2}\right)\left(\frac{3}{2}-\beta\right)\tilde{P}(z) = 0. \tag{22}$$

It is straightforward to check that the above equation is in the form of a hypergeometric differential equation,

$$z(1-z)\tilde{P}''(z) + [c_1 - (a_1+b_1+1)z]\tilde{P}'(z) - a_1 b_1 \tilde{P}(z) = 0 \tag{23}$$

with the parameters,

$$a_1 = 1 - \frac{\beta}{2}; \quad b_1 = \frac{3}{2} - \beta; \quad c_1 = \frac{3-\beta}{2}. \tag{24}$$

One can also get a similar second order equation for $\tilde{Q}(z)$. To this end, we first express $P'(z)$ in terms of $\tilde{Q}(z)$ and $\tilde{Q}'(z)$, i.e. in a form similar to equation (20). Multiplying equation (19) by $(1-\frac{\beta}{2})$ and equation (20) by $(1-\beta)$, and subtracting the latter resulting equation from the former, we get,

$$z\tilde{P}'(z) = (1-2\beta)\left(1-\frac{\beta}{2}\right)\tilde{Q} - [1-\beta-(2-\beta)z]\tilde{Q}'(z). \tag{25}$$

Taking a derivative of equation (20) and using equation (25), we get,

$$z(1-z)\tilde{Q}''(z) + \left[\frac{1-\beta}{2} - \frac{1}{2}(5-3\beta)z\right]\tilde{Q}'(z) - \left(1-\frac{\beta}{2}\right)\left(\frac{1}{2}-\beta\right)\tilde{Q}(z) = 0. \tag{26}$$

Clearly, this is also a hypergeometric differential equation of the form (23), but with a different parameter set,

$$a_2 = 1 - \frac{\beta}{2} = a_1, \quad b_2 = \frac{1}{2} - \beta = b_1 - 1, \quad c_2 = \frac{1-\beta}{2} = c_1 - 1. \tag{27}$$

### *3.1. Position distribution for $\beta \neq 1$*

The general solutions for equations (22) and (26) can be written in terms of the hypergeometric function ${}_2F_1(a,b,c;z)$ [55]. For $c_1 \neq 1$, i.e. for $\beta \neq 1$, these general solutions read,

$$P(z) = A_1\ [{}_2F_1(a_1,b_1,c_1;z)] + B_1 z^{1-c_1}\ [{}_2F_1(a_1-c_1+1, b_1-c_1+1, 2-c_1; z)] \tag{28}$$

$$Q(z) = A_2\ [{}_2F_1(a_2,b_2,c_2;z)] + B_2 z^{1-c_2}\ [{}_2F_1(a_2-c_2+1, b_2-c_2+1, 2-c_2; z)] \tag{29}$$

where $A_1, A_2, B_1, B_2$ are arbitrary constants. The case $\beta = 1$ is special, which we discuss later. To determine the constants $A_1, A_2, B_1, B_2$, we first use the original first order equations (19) and (20) which must be satisfied by the solution. Substituting equations (28) and (29) in (20) and using well known identities involving the hypergeometric function, we get, $B_2 = \frac{B_1}{1+\beta}$ and $A_2 = \frac{A_1(1-\beta)}{1-2\beta}$. Next, we impose the boundary condition (21). Once again, using properties of hypergeometric functions, we get

$$B_1 = \frac{2A_1}{\sqrt{\pi}} \frac{\Gamma(\frac{3-\beta}{2})\Gamma(\frac{1}{2}+\beta)}{(1-2\beta)\Gamma(\frac{1+\beta}{2})}. \tag{30}$$

To completely specify $\tilde{P}(z)$ we still need $A_1$ which can be determined using the normalization condition,

$$\int_{x_-}^{x_+} \mathrm{d}x\, P(x) = 1 \Rightarrow \int_0^{v_0/\mu} \mathrm{d}x\, \tilde{P}\left[\left(\frac{\mu x}{v_0}\right)^2\right] = \frac{1}{2}. \tag{31}$$

Fortunately, this integral can be performed analytically and yields,

$$A_1 = \frac{\mu}{2v_0}\left[{}_3F_2\left(\begin{matrix}\frac{1}{2} & \frac{3}{2}-\beta & 1-\frac{\beta}{2} \\ \frac{3}{2} & \frac{3-\beta}{2} & \end{matrix}; 1\right) - \frac{1}{\beta\sqrt{\pi}} \frac{\Gamma(\frac{3-\beta}{2})\Gamma(\beta-\frac{1}{2})}{\Gamma(\frac{1+\beta}{2})}\, {}_3F_2\left(\begin{matrix}\frac{1}{2} & 1-\frac{\beta}{2} & \frac{\beta}{2} \\ \frac{1+\beta}{2} & \frac{\beta}{2}+1 & \end{matrix}; 1\right)\right]^{-1} \tag{32}$$

where ${}_pF_q\left(\begin{smallmatrix}a_1,a_2,\ldots a_p \\ b_1,b_2,\ldots b_q\end{smallmatrix}; z\right)$ denotes the generalized hypergeometric function [55]. Finally, we can write an explicit expression for the stationary position probability distribution,

$$\begin{aligned} P(x) = A_1 \Bigg[ & {}_2F_1\left(1-\frac{\beta}{2}, \frac{3}{2}-\beta, \frac{3-\beta}{2}; \left(\frac{\mu x}{v_0}\right)^2\right) \\ & + \frac{2}{\sqrt{\pi}} \frac{\Gamma(\frac{3-\beta}{2})\Gamma(\beta+\frac{1}{2})}{(1-2\beta)\Gamma(\frac{\beta+1}{2})} \left(\frac{\mu x}{v_0}\right)^{\beta-1} {}_2F_1\left(\frac{1}{2}, 1-\frac{\beta}{2}, \frac{\beta+1}{2}; \left(\frac{\mu x}{v_0}\right)^2\right)\Bigg] \end{aligned} \tag{33}$$

where the normalization constant $A_1$ is given by equation (32). Note that, $P(x)$ is an even function of $x$ and its dependence on the flip rate $\gamma$ comes through the dimensionless parameter $\beta = \gamma/\mu$ only. $P(x)$ takes a particularly simple form for certain specific values of $\beta$,

$$P(x) = \begin{cases} \frac{\Gamma(\frac{3}{4})}{\sqrt{\pi}\Gamma(\frac{1}{4})} \frac{\sqrt{\mu v_0}}{\sqrt{|x|(v_0^2-\mu^2x^2)}} & \text{for} \quad \beta = \frac{1}{2} \\ \frac{\mu}{v_0}(1-\frac{\mu|x|}{v_0}) & \text{for} \quad \beta = 2 \\ \frac{6\mu}{5v_0}\left[1-5(\frac{\mu x}{v_0})^2 - \left(\frac{\mu|x|}{v_0}\right)^3\left((\frac{\mu x}{v_0})^2-5\right)\right] & \text{for} \quad \beta = 4. \end{cases} \tag{34}$$

One can also write an explicit expression for $Q(x)$ using equations (29) and (30),

$$\begin{aligned} Q(x) = \frac{A_1}{(1-2\beta)} \Bigg[ & (1-\beta)\, {}_2F_1\left(1-\frac{\beta}{2}, \frac{1}{2}-\beta, \frac{1-\beta}{2}; \left(\frac{\mu x}{v_0}\right)^2\right) \\ & + \frac{2}{\sqrt{\pi}} \frac{\Gamma(\frac{3-\beta}{2})\Gamma(\beta+\frac{1}{2})}{(1+\beta)\Gamma(\frac{\beta+1}{2})} \left(\frac{\mu x}{v_0}\right)^{\beta+1} {}_2F_1\left(\frac{1}{2}, 1-\frac{\beta}{2}, \frac{\beta+3}{2}; \left(\frac{\mu x}{v_0}\right)^2\right)\Bigg]. \end{aligned} \tag{35}$$

From equations (33) and (35) and using the relation (16) between $P(x)$ and $R(x)$ we can also calculate $P_i(x)$ individually in a straightforward manner. However, we do not give explicit expressions for them here.

Figures 2(a) and (c) show plots of $P(x)$ as a function of $x$ for different values of $\beta$ calculated from equation (33). We have also measured $P(x)$ from numerical simulations using standard Monte-Carlo methods for the orientation $\sigma$ and integrating equation (5*a*) by means of the Euler discretization scheme; the correspoding data are included in the figures. Similar to the 2-state RTP, the distribution shows two different behaviours near the boundary $x = x_\pm$

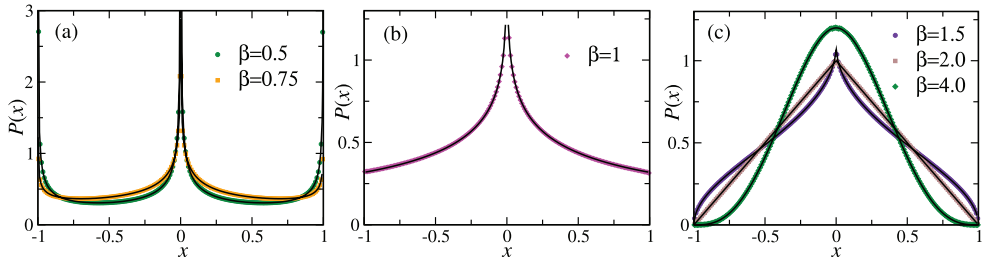


**Figure 2.** Stationary position distribution $P(x)$ as a function of $x$ for the 3-state model for (a) $\beta < 1$, (b) $\beta = 1$, and (c) $\beta > 1$. Here $v_0 = 1$ and $\mu = 1$. The symbols correspond to the data obtained from numerical simulations while solid lines are obtained from the exact result (see equations (33) and (46)).

depending on the value of $\beta$. Moreover, for $\beta < 1$, $P(x)$ also diverges near the origin $x = 0$ while it shows a cusp-like behaviour for large $\beta$. Such three-peak structures of the position distribution have been observed numerically earlier in the context of tracer particle motion in active gel [56, 57].

As discussed in the introduction, we find a shape transition in the stationary position distribution $P(x)$ as the 'activity' parameter $\beta$ is increased through $\beta = 1$. The non-Boltzmann shape of $P(x)$ for $\beta < 1$ is, in fact, a manifest signature of the active nature of the system in this regime. In the following we investigate the behaviour of $P(x)$ in more details and characterise this shape-transition at $\beta = 1$.

**Behaviour near $x = 0$.** To understand the behaviour of $P(x)$ near the origin we use the series expansion of the hypergeometric function ${}_2F_1(a, b, c; z)$ near $z = 0$,

$$ {}_2F_1(a,b,c;z) = 1 + \frac{ab}{c}z + \frac{ab(1+a)(1+b)}{2c(1+c)}z^2 + \mathcal{O}(z^3). \tag{36} $$

Using this expansion in equation (33), we have, near $x = 0$,

$$ P(x) \sim \begin{cases} B_1 \left(\frac{\mu}{v_0}x\right)^{\beta-1} & \text{for } \beta < 1 \\ A_1(1 - C_1 x^{\beta-1}) & \text{for } 1 < \beta < 3 \\ A_1(1 - C_2 x^2) & \text{for } \beta > 3 \end{cases} \tag{37} $$

where $B_1$ and $A_1$ are given respectively in equations (30) and (32) while $C_1$ and $C_2$ are given by

$$ C_1 = \frac{2}{\sqrt{\pi}} \frac{\Gamma(\frac{3-\beta}{2})\Gamma(\beta + \frac{1}{2})}{(2\beta - 1)\Gamma(\frac{\beta+1}{2})} \left(\frac{\mu}{v_0}\right)^{\beta-1}, \tag{38} $$

$$ C_2 = \frac{2\beta^2 + 6 - 7\beta}{2(\beta - 3)} \left(\frac{\mu}{v_0}\right)^2. \tag{39} $$

Clearly, for $\beta < 1$, $P(x)$ diverges near the origin. Note that, this divergence is integrable and the distribution remains normalized for all values of $\beta$. The emergence of this additional peak at the origin is a direct consequence of the presence of $\sigma_x = 0$ state: From equation (5*a*) it is clear that if $\sigma_x = 0$, the particle moves deterministically towards the origin, reaching it in a time $\sim \mu^{-1}$. If, additionally, the flip rate $\gamma$ is small, so that the typical time for changing its orientation $\gamma^{-1} > \mu^{-1}$ (i.e. $\beta < 1$), the particle spends a long time near the origin, thus giving rise to the diverging peak. For $\beta > 1$, on the other hand, $P(x)$ approaches a finite

value at $x = 0$. The approach also depends on the value of $\beta$ : for $1 < \beta < 3$, $P(x)$ has a cusp-like behaviour near the origin while for $\beta \geqslant 3$ it shows a quadratic behaviour, resembling a Gaussian around the origin. Indeed, in the diffusive limit, when $\gamma \to \infty$ and $v_0 \to \infty$ keeping $v_0^2/(2\gamma) = D$ fixed (as a consequence $\beta \to \infty$ in this limit), we find from equation (39) that $C_2 \to \mu/(2D)$. As a result, from the third line of (37), we recover the Boltzmann distribution $P(x) \sim \mathrm{e}^{-\mu/(2D)x^2}$ which actually holds for all $x$.

**Behaviour near $x = x_\pm$.** The position distribution $P(x)$ also shows an interesting behaviour near the boundaries $x = x_\pm$. As $P(x)$ is symmetric in $x$, it suffices to explore its nature near one boundary, say $x_+$. To characterise it we use the series expansion of ${}_2F_1(a, b, c; z)$ near $z = 1$. From equation (28), we have, for $z \to 1^-$,

$$\tilde{P}(z) \sim \begin{cases} (1-z)^{\beta-1} & \text{for } \beta < 3 \\ (1-z)^2 & \text{for } \beta > 3. \end{cases} \tag{40}$$

Hence, near $x = x_+$, we have the following behaviour of $P(x)$ :

$$P(x) \sim \begin{cases} (x_+ - x)^{\beta-1} & \text{diverges for } \beta < 1 \\ (x_+ - x)^{\beta-1} & \text{vanishes for } 1 < \beta \leqslant 3 \\ (x_+ - x)^2 & \text{vanishes for } \beta > 3. \end{cases} \tag{41}$$

A similar behaviour is seen also near $x = x_-$. Note that this 'freezing' for the leading behaviour for $\beta > 3$ occurs only for the three-state model, but not for the two-state model [24].

### 3.2. Position distribution for $\beta = 1$

As mentioned before, the case $\beta = 1$ is special. In this case, the differential equations (22) and (26) reduce to,

$$z(1-z)\tilde{P}''(z) + (1-2z)\tilde{P}'(z) - \frac{1}{4}\tilde{P}(z) = 0 \tag{42}$$

$$z(1-z)\tilde{Q}''(z) - z\tilde{Q}'(z) + \frac{1}{4}\tilde{Q}(z) = 0 \tag{43}$$

which correspond to two hypergeometric equations with $c_1 = 1$ and $c_2 = 0$, along with $a_1 = a_2 = b_1 = 1/2, b_2 = -1/2$. Equation (28) is not a general solution anymore as the two hypergeometric functions therein become identical. We use Mathematica to solve equations (42) and (43) and it turns out that the general solutions can be expressed in the form,

$$\tilde{P}(z) = \frac{2A_1}{\pi} K(1-z) + B_1 \mathcal{Q}_{-\frac{1}{2}}(2z-1) \tag{44}$$

$$\tilde{Q}(z) = A_2 z\, {}_2F_1\left(\frac{1}{2}, \frac{3}{2}, 2; z\right) + B_2\, G^{20}_{22}\left(\begin{matrix} \frac{1}{2} & \frac{3}{2} \\ 0 & 1 \end{matrix}; z\right). \tag{45}$$

Here $K(u)$ is the Legendre's complete elliptic integral of the first kind (see [58] and equation (19.2.8) in [55]), $G^{mn}_{pq}\left(\begin{smallmatrix} a_1, \ldots a_p \\ b_1 \ldots b_q \end{smallmatrix}; z\right)$ is the Meijer's G-function (see [58] and equation (16.17.1) in [55]) and $\mathcal{Q}_\nu(u)$ is the Legendre function of the second kind (see equation (14.3.7) in [55]).

To determine the arbitrary constants $A_1, A_2, B_1$ and $B_2$ we use the same strategy as in the previous section. First, we note that the solutions in equations (44) and (45) must satisfy the original first order equations (19) and (20) with $\beta = 1$ for all values of $z$. We then look at the behaviour of $\tilde{P}(z)$ and $\tilde{Q}(z)$ in equations (44) and (45) near $z = 0$. In this limit both $K(1-z)$

and $G^{20}_{22}\left(\begin{smallmatrix}\frac{1}{2} & \frac{3}{2}\\ 0 & 1\end{smallmatrix}; z\right)$ diverge logarithmically whereas the Legendre and hypergeometric functions approach a constant value. Substituting the series expansions of these functions back into equation (20) and comparing coefficients of $\ln z$ and different powers of $z$, we get, $B_2 = A_1$, and $A_2 = -\frac{\pi}{4}B_1$. It is also straightforward to check that equation (19) gives the same relation. We still have two independent constants $A_1$ and $B_1$. To determine these we use the boundary condition (21). Using the limiting behaviours of the special functions we have, for $z \to 1^-$, $\tilde{P}(z) - \tilde{Q}(z) = B_1 + \mathcal{O}(1-z)$ which immediately implies $B_1 = 0$ (see equation (21)). The last remaining constant $A_1$ can be determined from the normalization condition (31) and yields $A_1 = \frac{\mu}{\pi v_0}$. Finally, we have, for $\beta = 1$,

$$P(x) = \frac{2\mu}{\pi^2 v_0} K\left(1 - \frac{\mu^2 x^2}{v_0^2}\right), \quad \text{and} \quad Q(x) = \frac{\mu}{\pi v_0} G^{20}_{22}\left(\begin{smallmatrix}\frac{1}{2} & \frac{3}{2}\\ 0 & 1\end{smallmatrix}; \frac{\mu^2 x^2}{v_0^2}\right). \tag{46}$$

Figure 2(b) shows a plot of $P(x)$ for $\beta = 1$ together with the same obtained from numerical simulations. To understand the behaviour near the origin $x = 0$ and the boundaries $x = x_\pm$ we look at the series expansion of $P(x)$. Near $x = 0$, a logarithmic divergence is seen, $P(x) \sim -\ln x$. On the other hand, near the boundaries $x = x_\pm$, $P(x)$ approaches a constant value, $\lim_{x \to x_\pm} P(x) = \frac{\mu}{\pi v_0}$.

## 4. Conclusion

In this paper, we have solved exactly the stationary position distribution of a one-dimensional run-and-tumble (RTP) particle with three discrete internal states and subjected to an external harmonic potential. To our knowledge, this is the first exact solution with three states that generalizes the well-known result for the standard two-state RTP. We showed that the stationary state exhibits a rich behavior as a function of the single parameter $\beta = \gamma/\mu$ (where $\gamma$ represents the rate at which the internal state changes and $\mu$ is the stiffness of the trap). One of the interesting outcomes is that the stationary distribution undergoes a shape-transition at $\beta = 1$.

While we were able to characterise the stationary state of a three-state RTP in a harmonic trap exactly, it would be interesting to study the relaxational dynamics towards this stationary state, as was recently done for the two-state RTP [24]. It would also be natural to extend our studies to non-harmonic potentials, such as $U(x) \sim |x|^p$, with $p > 0$. Another natural extension would be to consider an RTP particle with more than three internal states. Finding even the stationary state of a general $n$-state RTP with $n > 3$ remains a challenging open problem.

## Acknowledgments

We acknowledge support from the project 5604-2 of the Indo-French Centre for the Promotion of Advanced Research (IFCPAR). SNM acknowledges the support from the Science and Engineering Research Board (SERB, government of India) under the VAJRA faculty scheme (Ref.VJR/2017/000110) during a visit to the Raman Research Institute in 2019, where part of this work was carried out. U B acknowledges support from Science and Engineering Research Board (SERB), India under Ramanujan Fellowship (Grant No. SB/S2/RJN-077/2018) and CNRS for a one month visit to LPTMS, Univ. Paris-Sud.

## ORCID iDs

Grégory Schehr https://orcid.org/0000-0001-6648-5213

## References


[1] Romanczuk P, Bär M, Ebeling W, Lindner B and Schimansky-Geier L 2012 *Eur. Phys. J. Spec. Top.* **202** 1
[2] Marchetti M C, Joanny J F, Ramaswamy S, Liverpool T B, Prost J, Rao M and Aditi Simha R 2013 *Rev. Mod. Phys.* **85** 1143
[3] Bechinger C, Di Leonardo R, Löwen H, Reichhardt C, Volpe G and Volpe G 2016 *Rev. Mod. Phys.* **88** 045006
[4] Ramaswamy S 2017 *J. Stat. Mech.* 054002
[5] Fodor É and Marchetti M C 2018 *Physica* A **504** 106
[6] Schweitzer F 2003 *Brownian Agents and Active Particles: Collective Dynamics in the Natural and Social Sciences* (Berlin: Springer)
[7] Berg H C 2004 *E. Coli in Motion* (Heidelberg: Springer)
[8] Cates M E 2012 *Rep. Prog. Phys.* **75** 042601
[9] Blair D L, Neicu T and Kudrolli A 2003 *Phys. Rev.* E **67** 031303
[10] Walsh L, Wagner C G, Schlossberg S, Olson C, Baskaran A and Menon N 2017 *Soft Matter* **13** 8964
[11] Toner J, Tu Y and Ramaswamy S 2005 *Ann. Phys., NY* **318** 170
[12] Kumar N, Soni H, Ramaswamy S and Sood A K 2014 *Nat. Commun.* **5** 4688
[13] Vicsek T, Czirók A, Ben-Jacob E, Cohen I and Shochet O 1995 *Phys. Rev. Lett.* **75** 1226
[14] Hubbard S, Babak P, Sigurdsson S Th and Magnússon K G 2004 *Ecological Modelling* **174** 359
[15] Fily Y and Marchetti M C 2012 *Phys. Rev. Lett.* **108** 235702
[16] Palacci J, Sacanna S, Steinberg A P, Pine D J and Chaikin P M 2013 *Science* **339** 936
[17] Slowman A B, Evans M R and Blythe R A 2016 *Phys. Rev. Lett.* **116** 218101
[18] Locatelli E, Baldovin F, Orlandini E and Pierno M 2015 *Phys. Rev.* E **91** 022109
[19] Schwarz-Linek J, Valeriani C, Cacciuto A, Cates M E, Marenduzzo D, Morozov A N and Poon W C K 2012 *Proc. Natl Acad. Sci. USA* **109** 4052
[20] Redner G S, Hagan M F and Baskaran A 2013 *Phys. Rev. Lett.* **110** 055701
[21] Stenhammar J, Wittkowski R, Marenduzzo D and Cates M E 2015 *Phys. Rev. Lett.* **114** 018301
[22] Solon A P, Fily Y, Baskaran A, Cates M E, Kafri Y, Kardar M and Tailleur J 2015 *Nat. Phys.* **11** 673
[23] Malakar K, Das A, Kundu A, Vijay Kumar K and Dhar A 2019 (arXiv:1902.04171)
[24] Dhar A, Kundu A, Majumdar S N, Sabhapandit S and Schehr G 2019 *Phys. Rev.* E **99** 032132
[25] Basu U, Majumdar S N, Rosso A and Schehr G 2019 *Phys. Rev.* E **100** 062116
[26] Solon A P, Cates M E and Tailleur J 2015 *Eur. Phys. J. Spec. Top.* **224** 1231
[27] Pototsky A and Stark H 2012 *Europhys. Lett.* **98** 50004
[28] Berke A P, Turner L, Berg H C and Lauga E 2008 *Phys. Rev. Lett.* **101** 038102
[29] Tailleur J and Cates M E 2009 *Eur. Phys. Lett.* **86** 60002
[30] Malakar K, Jemseena V, Kundu A, Vijay Kumar K, Sabhapandit S, Majumdar S N, Redner S and Dhar A 2018 *J. Stat. Mech.* 043215
[31] Basu U, Majumdar S N, Rosso A and Schehr G 2018 *Phys. Rev.* E **98** 062121
[32] Singh P and Kundu A 2019 *J. Stat. Mech.* 083205
[33] Kurzthaler C, Leitmann S and Franosch T 2016 *Sci. Rep.* **6** 36702
[34] Das S, Gompper G and Winkler R G 2018 *New J. Phys.* **20** 015001
[35] Caprinia L and Marconi U M B 2019 *Soft Matter* **15** 2627
[36] Sevilla F J, Arzola A V and Cital E P 2019 *Phys. Rev.* E **99** 012145
[37] ten Hagen B, Kümmel F, Wittkowski R, Takagi D, Löwen H and Bechinger C 2014 *Nat. Commun.* **5** 4829
[38] Takatori S C, De Dier R, Vermant J and Brady J F 2016 *Nat. Commun.* **7** 10694
[39] Deblais A, Barois T, Guerin T, Delville P H, Vaudaine R, Lintuvuori J S, Boudet J F, Baret J C and Kellay H 2018 *Phys. Rev. Lett.* **120** 188002
[40] Dauchot O and Démery V 2019 *Phys. Rev. Lett.* **122** 068002
[41] Angelani L 2013 *Eur. Phys. Lett.* **102** 20004
[42] Detcheverry F 2014 *Eur. Phys. J.* E **37** 114

[43] Slowman A B, Evans M R and Blythe R A 2017 *J. Phys. A: Math. Theor.* **50** 375601
[44] Angelani L and Garra R 2019 *Phys. Rev.* E **100** 052147
[45] Thompson A G, Tailleur J, Cates M E and Blythe R A 2011 *J. Stat. Mech.* P02029
[46] Paoluzzi M, Di Leonardo R and Angelani L 2013 *J. Phys.: Condens. Matter* **25** 415102
[47] Paoluzzi M, Di Leonardo R and Angelani L 2014 *J. Phys.: Condens. Matter* **26** 375101
[48] Horsthemke W and Lefever R 1984 *Noise-Induced Transitions: Theory and Applications in Physics, Chemistry and Biology* (Berlin: Springer)
[49] Klyatskin V I 1978 *Radiophys. Quantum El.* **20** 382
[50] Klyatskin V I 1977 *Radiofizika* **20** 562
[51] Lefever R, Horsthemke W, Kitahara K and Inaba I 1980 *Prog. Theor. Phys.* **64** 1233
[52] Hänggi P and Jung P 1995 *Adv. Chem. Phys.* **89** 239
[53] Pietzonka P, Kleinbeck K and Seifert U 2016 *New J. Phys.* **18** 052001
[54] Demaerel T and Maes C 2018 *Phys. Rev.* E **97** 032604
[55] Olver F W J, Olde Daalhuis A B, Lozier D W, Schneider B I, Boisvert R F, Clark C W, Miller B R, Saunders B V, Cohl H S and McClain M A *NIST Digital Library of Mathematical Functions* (http://dlmf.nist.gov)
[56] Ben-Isaac E, Fodor É, Visco P, van Wijland F and Gov N S 2015 *Phys. Rev.* E **92** 012716
[57] Razin N, Voituriez R and Gov N S 2019 *Phys. Rev.* E **99** 022419
[58] Gradshteyn I S and Ryzhik I M 1943 *Table of Integrals, Series, and Products* (New York: Academic)